RSC Advances

ROYAL SOCIETY OF CHEMISTRY

www.rsc.org/advances

Journal Name

ARTICLE

Characterization and lubrication performance of diesel soot nanoparticles as oil lubricant additives

Received 00th January 20xx,
Accepted 00th January 20xx

DOI: 10.1039/x0xx00000x

www.rsc.org/

Meng-fei Guo, Zhen-bing Cai*, Zu-chuan Zhang and Min-hao Zhu

Tribology Research Institute, Key Laboratory of Advanced Technologies of Materials (Ministry of Education), Southwest Jiaotong University, Chengdu 610031, China

Abstract: Diesel soot, a complex product of incomplete combustion, enters lubricant oils and acts as an additive. Thus, diesel soot significantly affects the performance of lubricants. In particular, the dispersion and concentration of diesel soot in lubricant media perform a key function. In this study, diesel soot was dispersed in PAO4 oil with 1wt % sorbitan monooleate (Span 80) as a dispersing agent. The chemical and structural features of three kinds of diesel soot (from loader soot, cement tanker soot, and bulldozer soot)were monitored by AFM, TEM, XRD, FT-IR, and Raman spectroscopy. The tribological behavior of different concentrations of loader soot provided with the optimal physicochemical properties and dispersion properties in comparison with other soot types was investigated using a UTM-2 tribometer. Tribology test results showed that diesel soot, as an additive to PAO4 oil, significantly reduced both friction and wear of steel balls and plates. The lubricant with a diesel soot concentration of 0.01wt % exhibited the optimal anti-wear performance, with a wear rate reduction of 75.2%. Bearing effects, as well as chemical and electrochemical actions were the main anti-wear mechanisms of diesel soot as an oil additive.

Keywords: Diesel soot; Additive; Nano-lubricant; Friction and wear

1 Introduction

Diesel engine combustion produces the highly carbonaceous material known as soot [1]. Part of soot retained in the engine lubricant is known as ‘‘engine’’ soot, which can significantly affect the performance of lubricants. The portion expelled to the environment via exhaust is known as “exhaust” soot, which is one of the important sources of atmospheric particulate matter with diameter of 2.5 micro metres or less(PM2.5). Diesel soot has been considered as a harmful substance to human health and the environment [2]. Moreover, diesel soot impairs engine performance by damaging cylinders and reducing the efficiency of power generation [3,4]. Liu et al. [5] found that increased soot affects not only the viscosity of oil but also the abrasive friction surface, causing mechanical damage. Therefore, the properties of diesel soot and tribological characteristics when particles are suspended in engine lubricant should be understood. The present work indicates that a comprehensive understanding of diesel soot engine tribology may be achieved by including the effects of physical structure and chemistry of soot [6-8]. Uy [9] has characterized diesel soot by using a variety of analytical techniques. Cai et al. [10] collected onion-like carbon nano-spheres from candle soot that were found to exert an efficient lubricant effect. Hu [11] indicated that the anti-friction properties of SAE 15W-40 formulated oil were strengthened by the addition of 2 wt % carbon black. Zhang et al. [12] studied the effects of different concentrations of tribological properties of graphene as lubricant additives and found that a graphene concentration of 0.02% exhibits the optimal anti-wear properties.

Several researchers believe that diesel soot perform a harmful action in the lubrication system[13-14]. The present study aims to explore the advantages of diesel soot by characterizing the morphology, structure, and composition of lubricant oils and finding the optimum concentration, thereby reducing wear mechanism for the anti-friction property.

2 Materials and methods

2.1 Soot collection

Three samples of diesel exhaust soot were collected from pipes leading to after-treatment systems of diesel vehicles for this study. All samples were collected at the location away from the exhaust port by 10 cm to 15cm and then stored in a thermostatic oven. Diesel vehicles include a loader, a concrete mixer truck, and a bulldozer (Fig.1). Among these vehicles, the loader engine is the most problematic because it often works under overloaded conditions. The amount of soot scraped

*Corresponding author: caizb@swjtu.cn, 610031
See DOI:10.1039/x0xx00000x

from the pipe was considerably larger than those of the other diesel vehicles. The concrete mixer truck frequently travels on flat roads comprising about 75% highway and 25% city driving. The service life of the bulldozer engine exceeds a decade, during which the engine has undergone several repairs. At present, this bulldozer works for 2 months to 3 months in a year. The soot samples and their associated detailed parameters are listed in Table 1.

(a) Loader (b) Concrete mixer truck (c) Bulldozer

Fig.1 Images of diesel engine vehicles

Table 1 Lists of samples and their associated parameters

Sample	Soot type	Engine type	Engine rated power (KW)	Engine rated speed (r/min)	Vehicles rated load (kg)	Engine service life (years)	Engine oil
Soot A	Exhaust	Loader	162	2800	5000	4	0#
Soot B	Exhaust	Concrete mixer truck	96	2300	4000	2	0#
Soot C	Exhaust	Bulldozer	382	2000	22000	10	0#

2.2 Characterization

Contact mode atomic force microscopy (AFM,SPI3800N, Japan) and transmission electron microscopy (TEM, JEM-2100F) were used to characterize the primary particle and aggregate size, as well as the bulk and surface microstructures of diesel soot. Diesel soot X-ray diffraction (XRD) measurements were performed using PANalytical X'Pert Pro X-ray diffractometer with nickel-filtered Cu Kα (1.54A) radiation as the X-ray source. The pattern was recorded in the 2θ range of 10° to 50°with a step size of 0.016.Fouriertransform infrared spectroscopy (FTIR, Nicolet 5700) was conducted using a Perkin-Elmer Spectrum One spectrometer in the range of 4000cm^{-1} to 500 cm^{-1} with a KBr pellet. Raman spectrum (Lab Ram HR) characterization utilized a 532 nm laser as excitation source. The zeta potential of particles in alcohol with a dispersant was measured by Zetasizer Nano-ZS90.To study the dispersion of diesel soot, three kinds of diesel soot were prepared and left to disperse for 360h.

2.3 Experimental methods

Tribology tests were conducted with a ball–plate contact wear model by using a UMT-2 testing machine. The upper ball sample was GCr15 steel(wt %:1.0 C,1.49 Cr,0.31 Mn,0.26 Si,0.009 P, 0.004 S) with a diameter of 9.525 mm and hardness of 766 HV fixed in a special clamp. The lower plate sample was an alloy cast iron RTCr2 (wt %,3.11 C,2.21 Si,0.50 Mn,1.63 Cr) with a size of 25mm × 12mm × 6 mm fixed in a square tank equipped with lubricating oil. The bottom of the tank was fitted with a heating device that can control the experimental temperature. In this study, different concentrations of diesel soot (Table 2) were added into PAO4 oil as lubricant for comparison. Given the high surface activity of nanoparticles, diesel soot is easy to aggregate [14,15]. To improve dispensability, 1wt % Span-80 ($C_{24}H_{44}O_6$, Chengdu, Changzheng Glass Co., Ltd.) was utilized as a dispersing agent. The mixed oil was stirred for over 10 min and then subjected to 15 min of ultrasonic vibration to create a uniform suspension in oil. The entire wear process was performed under the following conditions: normal load of 10N, sliding speed of 5mm/s, reciprocating sliding distance of 8mm, test time of 6000s, and temperature of 100°C.

After the wear test, specimens were cleansed with acetone and ethanol and then dried. The morphologies and tribo-chemistry of worn surfaces were analyzed through optical microscopy (OM, OLYMPUS BX60M), scanning electron microscopy (SEM ,JSM-7001F, JEOL, Tokyo, Japan), 2D profiler (NanoMap-D), energy dispersive X-ray spectroscopy (EDX, EDAX-7760 /68M), and Raman spectrum (Lab Ram HR) characterization.

Table 2 Concentrations of diesel soot of Western test

Test plan	PAO4+1wt %SP80+(*x*)wt % diesel soot												
Step 1	0	-	-	-	-	-	-	-	-	-	-	-	-
Step 2	-	0.001	0.005	-	-	0.01	-	-	0.05	0.1	0.5	1	5
Step 3	-	-	-	0.006	0.008	-	0.02	0.04	-	-	-	-	-

Journal Name

ARTICLE

3 Results and discussion

3.1Characterization of additive particles

The image in Fig.2 shows the HR-TEM and AFM images of primary particles and agglomerates of different diesel soot types. The particles are nearly circular in plane and elliptical in cross-section. The smallest unit of diesel soot is the primary particle [17] with sizes ranging from 20nm to 50nm (Fig.2a), 50nm to 70nm (Fig.2b) and 20nm to 70nm (Fig.2c). Soot A presents an evident layered structure. The agglomerates present a modest branching structure and fall in the size range of 30 nm to 150 nm (Fig.3).The AFM images did not only prove the TEM results but also showed a high degree of diesel soot agglomerates with a size of 2(Fig.3a), 10 (Fig.3b), and 5nm (Fig.3c).All three kinds of diesel soot are nanoparticles with relatively uniform particle size, and the primary particle size of Soot A is evenly distributed and relatively small.

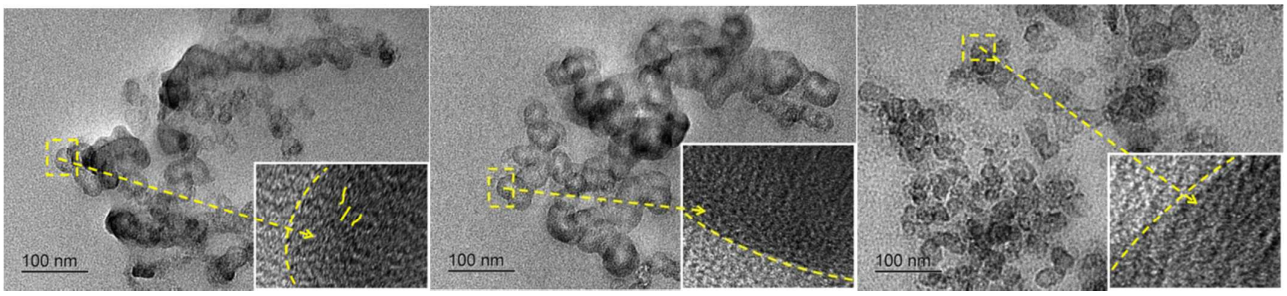

(a) Soot A (b) Soot B (c) Soot C

Fig.2 HR-TEM images of different diesel soot nanoparticles

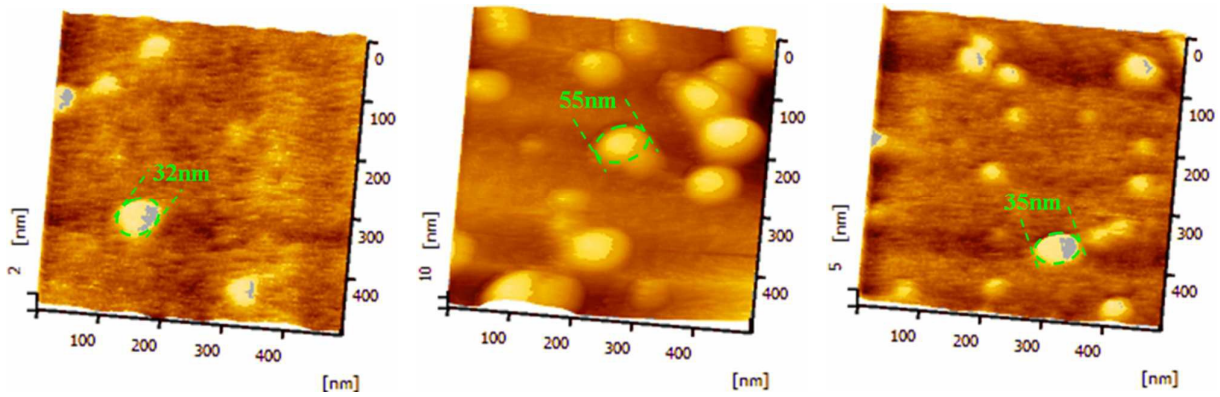

(a) Soot A (b) Soot B (c) Soot C

Fig. 3 AFM images of different diesel soot nanoparticles

The XRD pattern of graphite2H phase is known to exhibit three distinctive peak values in the 2θ range of 10° to 60°. These values are 26.8° (002), 42.3° (101), and 54.9° (102) according to the standard card PDF41-1487 database [18]. The XRD spectrum of diesel soot is shown in Fig.4a. The XRD results showed that strong diffraction peaks at 15° to 32° appeared in Soot A and Soot B, and weak diffraction peaks can be observed in Soot C. Why the peaks of soot C were weak? Although the diffraction measurement of a material was always accompanied by noise or background. But for Soot C, the reason maybe the test sample was not dry enough. These peaks suggest that the soot powder is amorphous in structure. The three kinds of diesel soot exhibited a relatively sharp diffraction peak in the vicinity of 2θ = 26.8° near the graphite

[002] crystal plane. The peak shape of Soot C is sharper, and the width at half-maximum of Soot C is narrower, indicating a higher graphitization degree of Soot C. In addition, Soot A presented significant diffraction peaks in the vicinity of 2θ = 44.6°, which is close to graphite [101] crystal plane. Thus, the degree of crystallinity of Soot A and Soot C is relatively better than that of Soot B [19-21].

As shown in the FT-IR spectrum (Fig.4b), the two medium absorption bands observed at 2970cm^{-1} to 2853cm^{-1} should be attributed to the stretching vibration of the CH bond of -CH_3 and -CH_2 groups. The band at 1739cm^{-1} corresponds to the functional group C=O. However, the peak of C=O is not detected in Soot C. The C=C absorption peak at 1635cm^{-1} is the standard peak of graphite, and the band at 1240cm^{-1} can be attributed to the absorption peak of C-O-C with an sp^2 structure.

The Raman spectrum (Fig.4c, excited by a 532 nm laser) showed the typical D (1250 cm^{-1} to 1450cm^{-1}) and G peaks (1500cm^{-1} to 1700cm^{-1}) of carbon crystal. Soot B exhibited the strongest D peak among the three kinds of diesel soot, indicating a high defect density in diesel soot. The ratio of D peak and G peak (I_D/I_G) follows a trend of Soot B>Soot A>Soot C, indicating that the extent of graphitization is Soot B<Soot A<Soot C. These findings were also verified by the XRD [22] test results.

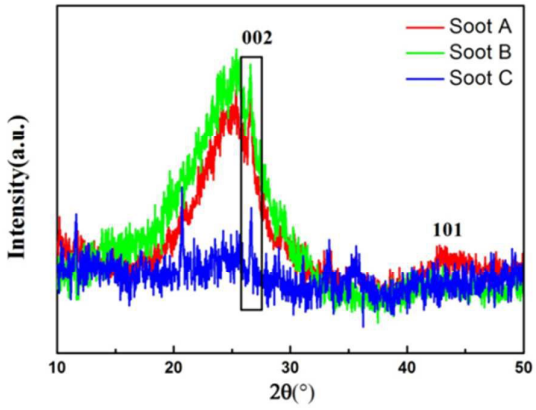

(a) XRD

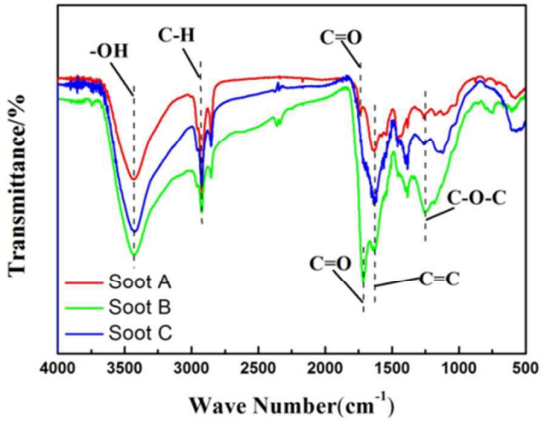

(b) FT-IR

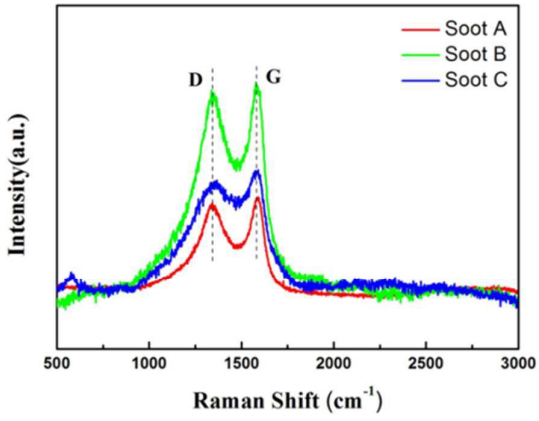

(c) Raman

Fig.4 XRD, FT-IR, and Raman spectra of different diesel soot types

The dispersion stability of diesel soot is shown in Fig.5. A 0.05 wt % solution was selected for comparison because the concentration of 0.01 wt % was very low for observation. The figure shows that the colour of the (2), (4), and (6) dispersion bottles added with dispersant is darker, indicating the improved effect of dispersion after dispersant addition. After being allowed to stand for 48h, the dispersion began to precipitate partially, except for the (2) bottle dispersion. However, the dispersion added with the dispersant remained darker. After 120h, the precipitation of dispersion was more evident and substantially reached a stable state. After 360h, the (2) bottle remained unchanged. The above phenomenon shows that Span80 effectively allows diesel soot and graphite to disperse well in the base oil. The Soot A dispersion with the added dispersant showed the optimum effect.

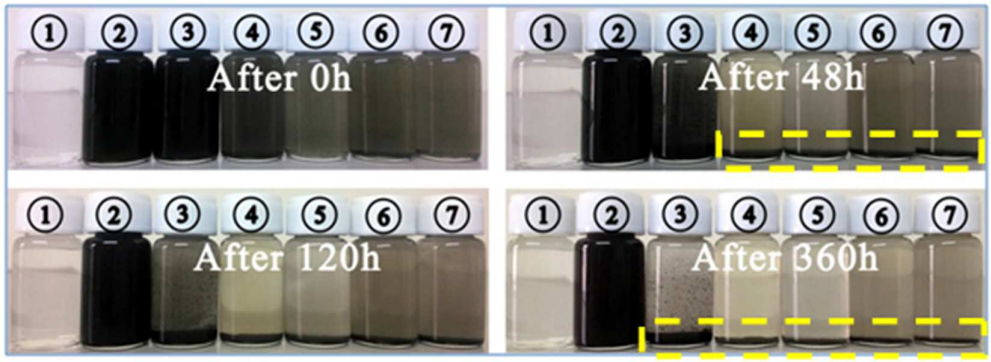

Fig.5 Optical images of dispersion property of different diesel soot types in base oil:

(1) PAO4, (2) PAO4+0.05 wt % Soot A +1 wt % SP, (3) PAO4+0.05 wt % Soot A, (4) PAO4+0.05 wt % Soot B +1 wt % SP,

(5) PAO4+0.05 wt % Soot B (6) PAO4+0.05 wt % Soot C +1 wt % SP, and(7) PAO4+0.05 wt % Soot C

In summary, the characterization results of the three kinds of diesel soot show that Soot A (the exhaust soot of loader) exhibits the optimal physical, chemical, and dispersion properties among the diesel soot types. Therefore, Soot A was selected as the concentration for testing the lubricating oil additives.

3.2 Friction and Wear

The average friction coefficients (COF) of different Soot A concentrations are compared in Fig.6. Each set of data represents an average of two repeat tests. The figure shows that dispersant addition (1wt %Sp80) and different additive concentrations of Soot A in PAO4 oil significantly reduce the friction coefficient in comparison with that of PAO4 base oil. For example, the COF of PAO4 was 0.57, and the value decreased to 0.12 after adding 0.01wt % concentration of Soot A. However, after adding the dispersant and additive, COF initially increased (0wt % to 0.001wt %), subsequently decreased (0.001wt % to 0.01wt %), and then remained virtually unchanged (0.01wt % to 5wt %). In addition, COF decreased by different degrees with the addition of different concentrations of Soot A. This finding showed that a competition of dispersants and additives occurred in the lubrication process, and the concentration of Soot A exerted a major effect on friction.

Considering that the wear amount of balls is markedly lower than that in plates, worn plate scars were analysed in this study. The wear rate can be defined as the volume loss, V (mm^3) on per loading force, F (N) and total sliding distance, S (mm).

$$\text{Wear rate} = {}^{V}/_{F * S} \quad (1)$$

Volume loss (*V*) can be calculated as:

$$V = A * d \quad (2)$$

where *A* is the average cross section area of the wear track and d is single sliding distance.

Total sliding distance (S) can be calculated as:

$$S = v * t \quad (3)$$

Where *v* is sliding speed and *t* is test time.

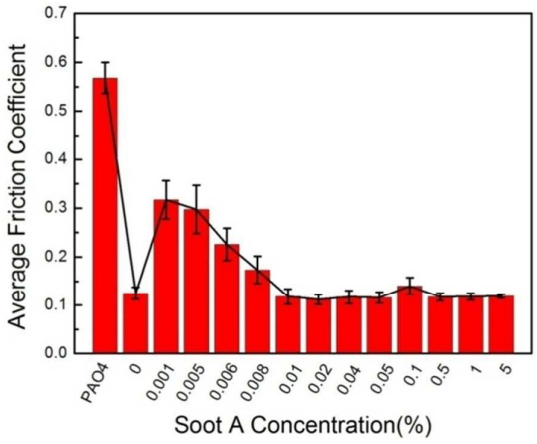

Fig.6 Average friction coefficient with different Soot A concentrations

The image in Fig.7 shows the maximum width and depth of worn plates under the conditions of adding different Soot A concentrations in PAO4 base oil. The highest value of maximum width and depth appears at the condition of PAO4 lubrication, and the lowest value appears with the addition of0.01wt % Soot A in PAO4 base oil. These results are consistent with the results of wear rate in Fig.8, and a similar trend is observed in Fig.7 and Fig.8. The wear rate and the maximum width and depth are significantly reduced after the addition of Soot A. For example, the maximum reduction of wear rate is 76% at the optimal concentration of 0.01wt %.This result may be ascribed to the formation of a protective film on the surface of the friction pair, which separates the friction pair of direct contact to reduce the wear rate. The lubricant achieving the optimum effect at the concentration of 0.01wt % may be ascribed to competition of additives and dispersant in the friction process, thereby achieving a mutually beneficial situation at a concentration of 0.01wt % Soot A. Notably, the wear rate at the concentration of 0wt % (1wt %SP80) is less than that at 0.001 and 0.005 wt %. This finding is attributed to the low soot concentration, which is insufficient for forming stable protective films. Extremely high soot concentration is

known to increase wear and tear [4,23-25]. However, in this study, the wear rate at a high concentration remains low, which may be ascribed to the dispersion producing considerable precipitation in the course of friction when the concentration exceeds 0.05%.

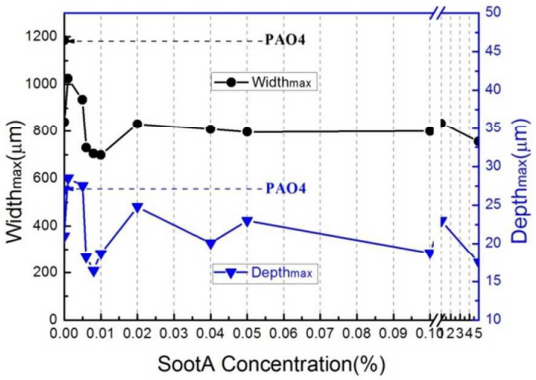

Fig.7 Maximum width and depth of worn plates

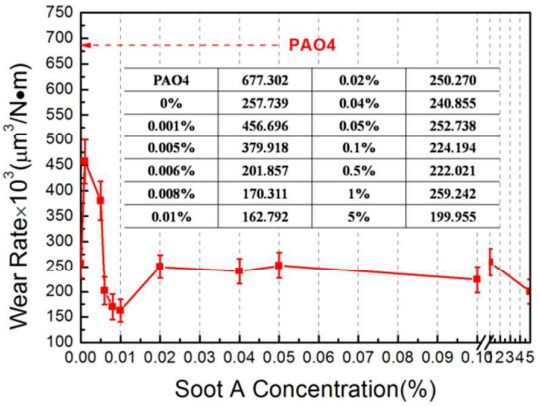

PAO4	677.302	0.02%	250.270
0%	257.739	0.04%	240.855
0.001%	456.696	0.05%	252.738
0.005%	379.918	0.1%	224.194
0.006%	201.857	0.5%	222.021
0.008%	170.311	1%	259.242
0.01%	162.792	5%	199.955

Fig.8 Wear rate of worn plates

The SEM morphologies of worn surfaces and EDX spectroscopy of balls are shown in Fig.9. As can be seen in Fig.9a to Fig.9c, the worn area with PAO4 lubrication is relatively large with metallic luster, and the worn plate surface displays a number of clear grooves and considerably larger “peeling pits”(zones surrounded by white cracks).These results indicated that severe scuffing occurred in this case. With the addition of different concentrations of Soot A in PAO4 base oil (Fig.9d to Fig.9l), the worn ball areas were significantly reduced. Moreover, despite the abundant presence of “peeling pits” and grooves in the worn plate surface, the defects become relatively shallow and narrow. Thus, Soot A additive provides anti-wear property to a certain degree. In particularly, at a concentration of 0.01wt % (Fig.9g to Fig.9i), the ball shows the minimum wear area, and the plate only presents slight furrows. This finding demonstrates that the concentration of 0.01 wt% presents the optimum effect. Simultaneously, EDX spectroscopy (Fig.9d, Fig.9g, and Fig.9i) results showed that the content of carbon and oxygen in worn areas are higher, and the value of oxygen at the “accumulation” (area revolved by white line) zone increased significantly. This finding indicated that a chemical reaction occurred during friction process. In addition, “accumulation” is likely to include oxidation products and is more inclined to combine with soot. These results may explain the anti-wear of the base oil added in PAO4 base oil.

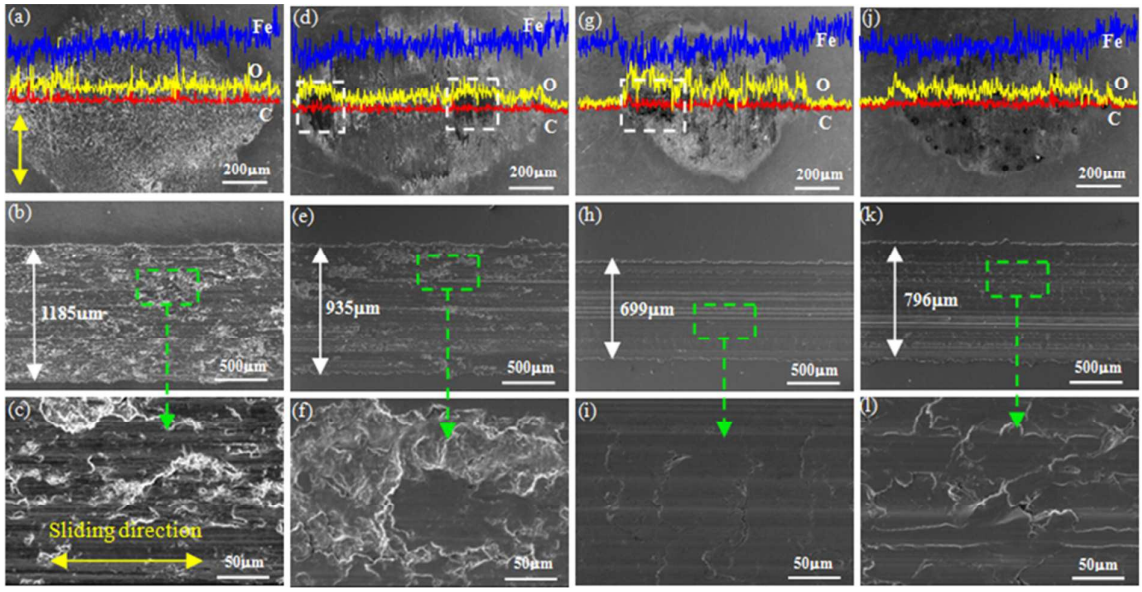

Fig.9 SEM micrographs of worn surfaces and EDX spectroscopy of balls

(a), (b), and (c) PAO4; (d), (e), and (f) 0.005wt % Soot A;(g), (h), and (i) 0.01 wt % Soot A;(j), (k), and (l) 0.05 wt % Soot A

The image in Fig.10a shows that the wear scar of ball presents an oval shape instead of a circular shape and the edge of wear scar (I) was worn lightly, whereas the middle was worn severely (II). The explanation is shown inFig.10c: (i) the contact area of ball and plate in the X direction is larger than those in the Y direction, because the plate material is worn off in the Y direction. (ii) According to the calculation results of Hamilton and Goodman [26], the stress distribution on the ball-on-plate contact surface under full slipping state is the outer part of the contact zone, which showed the minimum shear stress, whereas the middle zone showed the maximum shear stress. At the same time, EDX spectroscopy (Fig.10a, Fig.10b) indicates that the content of oxygen is significantly increased in the worn area and that the value of oxygen at the "accumulation" zone (Fig.10a) is the highest. This finding indicates that an electrochemical reaction occurred in the worn area and that the production is easily attached to the worn surface. The Fig.10b image also shows the hardness distribution of worn plates. The hardness values were in the order PAO4 (worn area)>0.01wt % Soot A additive oil (worn area)>substrate (unworn).Friction is known to result in the hardening of the tribo-pair and cause the plastic deformation layer to achieve increased hardness. Evidently, the additives reduced the hardness of the friction surface, because additives can promote the formation of an oil film. Another possibility is that a protective film with high carbon content was formed in oil-containing additives [27,28].

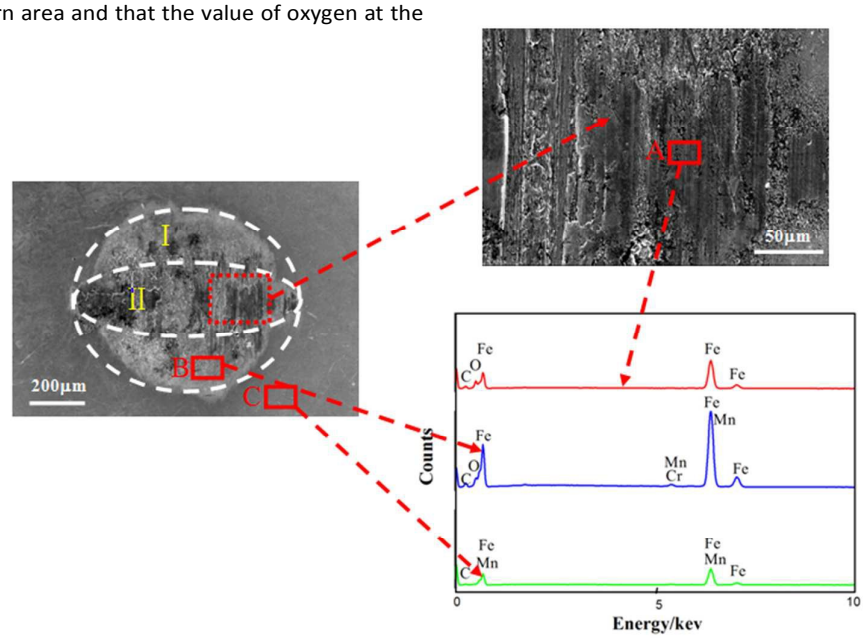

(a) SEM micrographs of worn ball scar and EDX spectroscopy

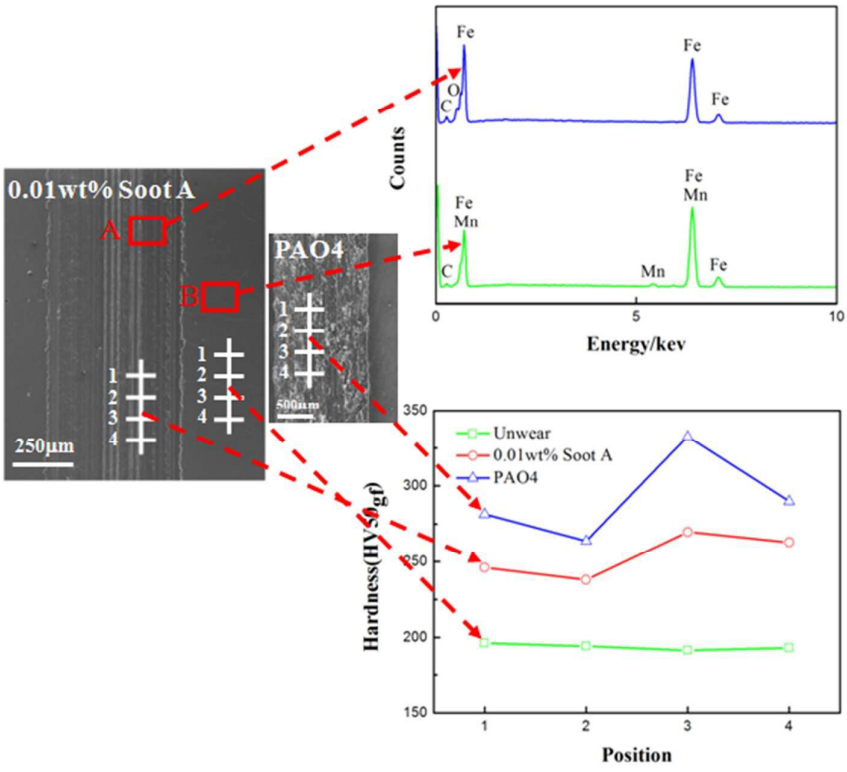

(b) SEM micrographs of worn plate scar, EDX spectroscopy and hardness distribution

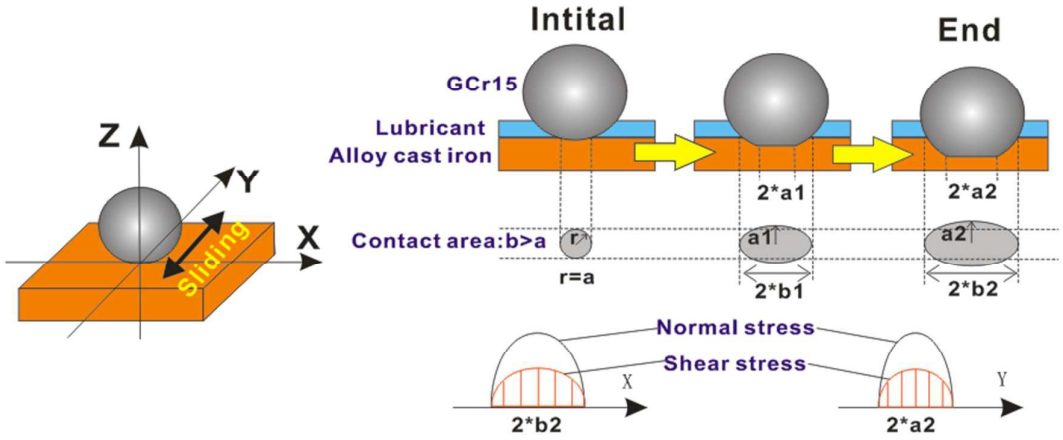

(c) Schematic of wear progress

Fig.10 SEM, EDX, hardness distribution of wear scars, and wear mechanism

The Raman spectrum of the worn surface of balls and plates is shown in Fig. 11. The D and G characteristic peaks of graphite crystals were detected in the worn surface of balls and plates. In addition, the relative intensity of the D and G peaks of the worn ball surface was evidently stronger than those of plates. Notably, the relative intensity of the D peak was significantly stronger than that of the G peak under the condition of 0.01wt % soot lubrication addition. Therefore, we can infer that a physical film was absorbed on the worn surface of balls and plates during lubrication. In addition, the relative intensity of the G peak is strengthened because of the enhanced contribution of graphite key in diesel soot, and the strengthening of D peaks may explain the increase in doping amount or the change in dipole moment [29]. At the same time, the Raman spectrum of the worn surface of balls and plates show a clear characteristic peak of Fe_3O_4 at 661cm^{-1}, and the characteristic peak of α-Fe_2O_3 appears at 298 and 405 cm^{-1} [10]. This finding may be ascribed to the occurrence of friction chemical reaction during the friction process, and

forming iron oxides that can also protect the contact surface of ball–plate.

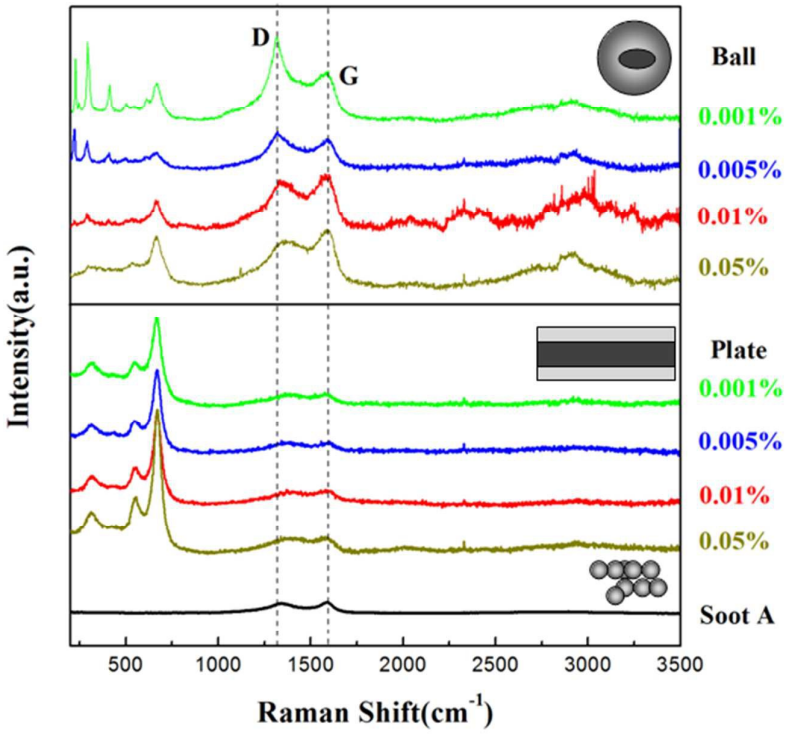

Fig.11 Raman spectroscopy of worn balls and plates

3.3 Lubrication mechanism

The tribological results of this research show that diesel soot displays excellent friction-reducing and anti-wear properties as additives in PAO4, with the optimum effect observed at the concentration of 0.01wt %. This finding compelled us to investigate the lubrication mechanism.

The zeta potential of different diesel soot particles in alcohol is shown in Table 3. The surface of the three kinds of diesel soot particles carry a small amount of negative charge, This charge may be ascribed to a small amount of oxygen-containing polar group on the surface [30].

Table3 Zeta potential of different diesel soot particles

Sample	Soot A	Soot B	Soot C
Zeta potential(mV)	−0.516	−0.994	−0.831

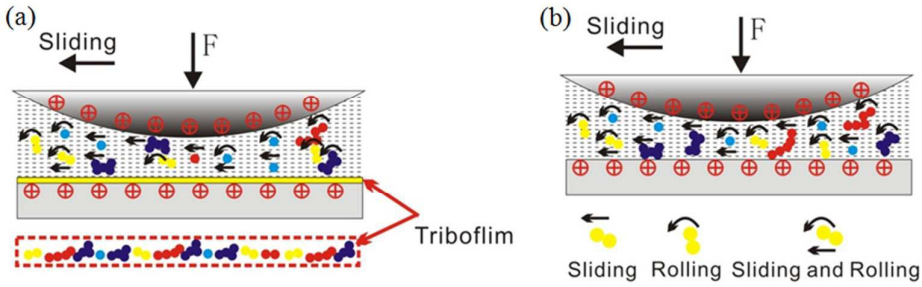

Fig.12 Lubrication mechanism diagram of diesel soot in PAO4 base oil

As seen from HR-TEM (Fig.2) and AFM (Fig.3) images, diesel soot is composed of nanoparticles with spherical and approximate ellipsoid structure. During the sliding process, the metal surface carries a positive charge because of the low-energy electrons emitted from contact convex points on the metal surface [31]. Diesel soot with a negative charge (Table 3) can be adsorbed onto the surface of a sliding pair to form a protective layer (Fig.12a). In addition, part of diesel soot is exfoliated by shear force to generate isolated graphite sheets [32]. This formation was proven by the enhanced contribution

of the graphite key (Fig.11). As a result, graphite and magnetite can form a composite film (Fig.12a) that effectively reduces friction and wear [33,34], as can be obtained from the results of the EDX spectrum (Fig.9d, Fig.9g, Fig.9j, and Fig.11).At low concentrations of diesel soot (<0.01wt %), the main mechanism of weak antifriction wear involves the increase in surface defects (Fig.11), which in turn results in the ability of forming a graphite–magnetite film. At the same time, spherical and ellipsoidal structures easily roll and slide under an external force. Under shear force, diesel soot moves between contact surfaces to prevent the direct contact of friction pair. The motion is similar to that of bearing balls to achieve anti-friction anti-wear effect [35-37] (Fig.12b). At a diesel soot concentration of 0.01wt %, the optimal antifriction wear is attributed to the stronger ability of formation of graphite–magnetite film (Fig.9g, Fig.11), and the motions reach the optimum state. At high concentrations (>0.05wt %), given dispensability reasons, a considerable amount of precipitate adhering to the surface changes the contact manner to achieve the wear reduction effect. However, this mechanism does not belong to the above-described anti-friction conditions.

In conclusion, the particle size of diesel soot, dispersion stability, surface charge, electrochemical action, and concentrations of diesel soot are important factors influencing lubrication.

Conclusions

Three kinds of diesel soot were easily prepared from pipes leading to after-treatment systems of diesel vehicles.

(a) Diesel soot particles show almost circular in plane and elliptical in cross-section with a size of 20nm to 70nm, which demonstrates a degree of internal chaos turbostratic graphitization. The dispersion of diesel soot indicated that Soot A exhibits better dispensability than other diesel soot types when Sp80 was utilized as a dispersant.

(b) Diesel soot as additive in PAO4 oil displays excellent friction-reducing and anti-wear properties, with the optimum effect observed at the concentration of 0.01wt %.

(c) Magnetite–graphite composite tribofilm occurred in the wear scars. Through a mechanism of rolling, sliding, and the composite motion of rolling and sliding between the friction pair, the direct contact of friction pair is blocked to achieve excellent friction reduction and anti-wear effect.

(d) The particle size, dispersion stability, surface charge, electrochemical action, and concentrations of diesel soot are important factors influencing lubrication properties.

Acknowledgements

This study was supported by National Science Foundation of China (51375407 and U1530136), The authors thank Dr. Wen Yue from China University of Geosciences in Beijing for providing the PAO4 oil. And thank Dr. Jin-fang Peng from Southwest Jiaotong University for SEM sample preparation and partial EDX analysis.

References

1 Clague A D H, Donnet J B, Wang T K, et al. A comparison of diesel engine soot with carbon black 1[J]. Carbon. 1999, 37, 1553–1565.
2 Bhowmick H, Majumdar S K, Biswas S K. Influence of physical structure and chemistry of diesel soot suspended in hexadecane on lubrication of steel-on-steel contact[J]. Wear. 2013, 300, 180–188.
3 Taylor R I, Mainwaring R, Mortier R M. Engine Lubricant Trends Since 1990[J]. Proceedings of the Institution of Mechanical Engineers Part J Journal of Engineering Tribology. 2005, 219, 331-346.
4 Green D A, Lewis R. The effects of soot-contaminated engine oil on wear and friction: A review[J]. Proceedings of the Institution of Mechanical Engineers Part D Journal of Automobile Engineering. 2008, 222, 1669-1689.
5 Liu H G, Li W D, Wang D, et al. Study on the soot in lubricating oil for railway locomotive diesel engine. China.Rail.Science. 2007, 22, 73-77.
6 Chi09as-Castillo F, Spikes H A. The Behavior of Diluted Sooted Oils in Lubricated Contacts[J]. Tribology Letters. 2004, 16, 317-322.
7 Ryason P R, Chan I Y, Gilmore J T. Polishing wear by soot[J]. Wear. 1990, 137, 15–24.
8 Berbezier I, Martin J M, Kapsa P. The role of carbon in lubricated mild wear[J]. Tribology International. 1986, 19, 115–122.
9 Uy D, Ford M A, Jayne D T, et al. Characterization of gasoline soot and comparison to diesel soot: Morphology, chemistry, and wear[J]. Tribology International. 2004, 198–209.
10 Wei J, Cai M, Zhou F, et al. Candle Soot as Particular Lubricant Additives[J]. Tribology Letters. 2014, 53, 521-531.
11 George, S., Balla, S., Gautam, M.: Effect of diesel soot contaminated oil on engine wear. Wear. 2007, 262, 1113–1122.
12 Zhang Wei, Zhou Ming, Zhu Hongwei, et al. Tribological properties of oleic acid-modified graphene as lubricant oil additives[J]. Journal of Physics D Applied Physics. 2011, 44, 4329-4334.
13 Dairene Uy,Monica A. Ford, Douglas T. Jayne, et al. Characterization of gasoline soot and comparison to diesel soot: Morphology, chemistry, and wear[J]. Tribology International,2014,80, 198–209
14 Mainwaring, R., "Soot and Wear in Heavy Duty Diesel Engines", SAE 971631, 1997.
15 Xiao H, He J, Yu L, et al. Preparation and tribological properties of fluorosilane surface-modified lanthanum trifluoride nanoparticles as additive of fluoro silicone oil[J]. Applied Surface Science. 2014, 316, 515–523.
16 Chunli Zhang, Shengmao Zhang, Laigui Yu, et al. Preparation and tribological properties of water-soluble copper/silica nanocomposite as a water-based lubricant additive[J]. Applied Surface Science. 2012, 259, 824-830.
17 Koylu U O. Fractal and projected structure properties of soot aggregates[J]. Combustion & Flame. 1995, 100, 621–633.
18 Sadezky A, Muckenhuber H, Grothe H, et al. Raman microspectroscopy of soot and related carbonaceous materials: Spectral analysis and structural information[J]. Carbon. 2005, 43, 1731–1742.
19 Eswaraiah V, Sankaranarayanan V, Ramaprabhu S. Graphene-based engine oil nanofluids for tribological applications.[J]. Acs Appl Mater Interfaces. 2011, 3, 4221-7.

20 M Patel, CL Azanza Ricardo, P Scardi, et al. Morphology, structure and chemistry of extracted diesel soot—Part I: Transmission electron microscopy, Raman spectroscopy, X-ray photoelectron spectroscopy and synchrotron X-ray diffraction study[J]. Tribology International. 2012, 5, 29–39.
21 Li Xiuti, Yao Zhitong, Sun Jie, et al. Study on preparation and surface modification of precipitated silica obtained from fly ash [J]. Functional Materials. 2010, 41, 939-942.
22 Ferrari A C, Meyer J C, Scardaci V, et al. Raman Spectrum of Graphene and Graphene Layers[J]. Physical Review Letters. 2006, 97, 3831-13840.
23 Dennis A J, Garner C P, Taylor D H C. The Effect of EGR on Diesel Engine Wear, 1999, SAE Paper No. 1999-01-0839.
24 Kim C, Passut C A, Zang D M. Relationships Among Oil Composition Combustion-Generated Soot, and Diesel Engine Valve Train Wear, 1992, SAE 922199.
25 Green D A, Lewis R, Dwyer-Joyce R S. Wear effects and mechanisms of soot-contaminated automotive lubricants[J]. Proceedings of the Institution of Mechanical Engineers Part J Journal of Engineering Tribology. 2006, 220, 159-169.
26 Hamilton G M, Goodman L E. The Stress Field Created by a Circular Sliding Contact[J]. Asme J.appl.mech. 1966, 33, 371-376.
27 Ratoia M, Anghela V, Bovingtonb, et al. Mechanisms of oiliness additives. Tribology International. 2000, 33, 241–247.
28 Ernesto A, Mazuyer D, Cayer-Barrioz J. The Combined Role of Soot Aggregation and Surface Effect on the Friction of a Lubricated Contact[J]. Tribology Letters. 2014, 55, 329-341.
29 Li Liuhe, Xia Lifang, Zhang Haiquan, et al. Tribological Properties and the Current State of Tribological Investigation of Diamond-like Carbon Films [J]. Tribology. 2001, 21, 76-80.
30 Gao Chuanping, Wang Yanmin, Xiang Longhua, et al.Tribochemical Properties of Fe3O4 Nanoparticles with Hexagonal Morphology in Lubricating Oil [J]. Journal of the Chinese Ceramic Society. 2013, 41, 1339-1346.
31 Antusch S, Dienwiebel M, Nold E, et al. On the tribochemical action of engine soot [J]. Wear.2010, 269, 1-12.
32 Joly-Pottuz L, Matsumoto N, Kinoshita H, et al. Diamond-derived carbon onions as lubricant additives[J]. Tribology International. 2008, 41, 69–78.
33 Scharf T W, Prasad S V. Solid lubricants: a review[J]. Journal of Materials Science. 2013, 48, 511-531.
34 Hirata A, Igarashi M, Kaito T. Study on solid lubricant properties of carbon onions produced by heat treatment of diamond clusters or particles[J]. Tribology International. 2004, 37, 899–905.
35 Li X S, Zhao Y B, Wu W, et al. Synthesis and characterizations of graphene–copper nanocomposites and their antifriction application. J. Ind. Eng.Chem. 2014, 20, 2043-2049.
36 Bucholz E W, Phillpot S R, Sinnott S B. Molecular dynamics investigation of the lubrication mechanism of carbon nano-onions[J]. Computational Materials Science. 2012, 91–96.
37 Zhang L L, Pu J B, Wang L P, et al. Frictional dependence of graphene and carbon nanotube in diamond-like carbon/ionic liquids hybrid films in vacuum. Carbon. 2014, 80, 734-735.